Journal of Materials Chemistry B

ROYAL SOCIETY OF CHEMISTRY

PERSPECTIVE

View Article Online
View Journal | View Issue

Cite this: J. Mater. Chem. B, 2023, 11, 6994

Nanomaterials enabled and enhanced DNA-based biosensors

Stefen Stangherlin and Juewen Liu *

DNA has excellent molecular recognition properties. At the same time, DNA has a programmable structure, high stability, and can be easily modified, making DNA attractive for biosensor design. To convert DNA hybridization or aptamer binding events to physically detectable signals, various nanomaterials have been extensively exploited to take advantage of their optical and surface properties. A popular sensing scheme is through the adsorption of a fluorescently-labeled DNA probe, where detection is achieved by target-induced probe desorption and fluorescence recovery. Another method is to use DNA to protect the colloidal stability of nanomaterials, where subsequent target binding can decrease the protection ability and induce aggregation; this method has mainly been used for gold nanoparticles. This Perspective summarizes some of our work in examining the sensing mechanisms, and we articulate the importance of the understanding of DNA/surface and target/surface interactions for the development of practical DNA-based biosensors.

Received 14th May 2023,
Accepted 11th July 2023

DOI: 10.1039/d3tb01100c

rsc.li/materials-b

Introduction

DNA hybridization probes and aptamers can collectively detect essentially any type of target molecule. Since DNA oligonucleotides are chemically synthesized, they can be conveniently modified at specific sites during synthesis with fluorophores and other functional groups to introduce various types of chemistry. Interfacing DNA with nanomaterials has produced numerous biosensors and hybrid materials.[1–5] For biosensors, two types of nanomaterials have received the most attention: gold nanoparticles (AuNPs) and graphene oxide (GO). The vivid color change of DNA-functionalized AuNPs from red to blue upon assembly by hybridization, initially reported by the Mirkin group in 1996,[6] has inspired many subsequent bioanalytical studies in this direction.[7–9] In 2004, Li and Rothberg found that citrate-capped AuNPs can distinguish single-stranded (ss) and double-stranded (ds) DNA based on their difference in the protection of the colloidal stability of AuNPs.[10,11] The simplicity

Department of Chemistry, Waterloo Institute for Nanotechnology, Waterloo, ON, N2L 3G1, Canada. E-mail: liujw@uwaterloo.ca

Stefen Stangherlin

Stefen Stangherlin received his MSc degree from Wilfrid Laurier University in 2021, where he studied the molecular determinants of substrate and inhibitor binding of a virulent enzyme from Neisseria gonorrhoeae in the lab of Dr Anthony J. Clarke. He had previously received a BSc degree from Wilfrid Laurier University in 2019, where he worked under the supervision of Dr Vladimir Kitaev in the synthesis of gold and silver nanoparticles. Stefen is currently pursuing a PhD degree at the University of Waterloo in the lab of Prof. Juewen Liu.

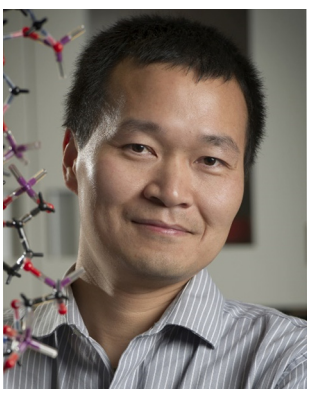

Juewen Liu

Prof. Juewen Liu received his PhD degree from the University of Illinois at Urbana-Champaign in 2005. He is currently a professor of chemistry at the University of Waterloo, and holds a University Research Chair position. He is a College member of the Royal Society of Canada (RSC). He serves as a Section Editor for Biosensors & Bioelectronics, and a Contributing Editor for Trends in Analytical Chemistry. He is interested in metal-dependent DNAzymes, aptamers, biointerface sciences, and nanozymes. He has published over 400 papers, receiving over 39 000 citations with an H-index of 94.

of this method has also attracted a lot of follow-up work to develop label-free colorimetric biosensors. In 2009, Yang and coworkers adsorbed fluorescently-labeled DNA and aptamer probes to GO, leading to nearly fully quenched fluorescence.[12] When complementary DNA (cDNA) or aptamer targets were added, a rapid fluorescence enhancement was observed. The work on GO has since inspired efforts to find a plethora of nanomaterials, from MoS_2/WS_2,[13] various metal oxides[14] and carbon-based nanomaterials,[15] to metal nanoparticles.[16] They all followed a similar reaction scheme of fluorescence quenching and dequenching.

However, not all nanomaterials work the same way, and each nanomaterial has its own interaction mechanism with DNA. A lot of biosensor papers focused on sensor performance but neglected the materials and surface chemistry of the employed nanomaterials. After over 20 years of development, it is now a good time to critically understand the status of the field. While many reviews exist on DNA/nanomaterial based biosensors,[1,9,17,18] our goal here is different. We aim to critically evaluate DNA/nanomaterial interfaces and interactions, and its effect on sensing. In this Perspective, we describe some of our own fundamental work in nanomaterial/DNA-based biosensors. We focus most of our discussion on non-modified nanomaterials, where direct adsorption of DNA is critical for signal generation. In many cases, the observed signal change did not reflect intended DNA hybridization or aptamer binding reactions. Instead, signal change could be due to the adsorption of target molecules directly to the nanomaterials. In the end, some future perspectives are discussed.

Interactions between DNAs and nanomaterials

With a negatively charged phosphate backbone and the four types of nucleobases, DNA can be adsorbed to a diverse range of nanomaterials based on various intermolecular or surface forces. For example, ssDNA oligonucleotides can be adsorbed to gold surfaces *via* strong DNA base coordination. Among the four bases, adenine has the strongest affinity and thymine has the weakest affinity.[19,20] However, thymine adsorption is still much stronger than a typical hydrogen bond or base pairing interactions. Thus, once a DNA strand is adsorbed to a gold surface, it is difficult to desorb it by adding its cDNA. For this reason, DNA-functionalized gold electrodes need to be backfilled with 6-mercaptohexanol (MCH) to disrupt the nucleobase/gold interactions.[21,22] Otherwise, DNA hybridization cannot be achieved. Indeed, functionalizing AuNPs with thiolated DNA does not require MCH, since here DNA can use its own thiol group to achieve this purpose when a high density of DNA is attached.[23]

DNA is adsorbed to GO using π–π stacking and hydrogen bonding,[15] and a high concentration of urea (a hydrogen bond disruptor) can efficiently remove DNA from the GO surface.[24] This type of adsorption is weaker than that on a gold surface, and adsorbed DNA can be displaced by adding other molecules.[12] Finally, DNA can use its phosphate backbone to interact with many metal oxide surfaces, although DNA bases may also be involved in adsorption.[14,25] Depending on the type of metal in the metal oxides, the adsorption strength can vary

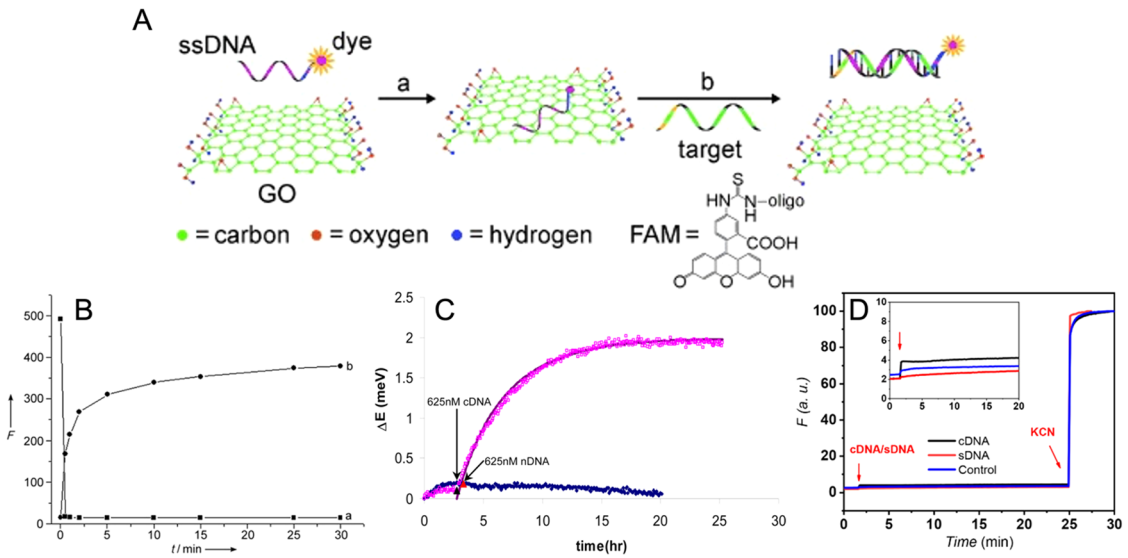

Fig. 1 (A) Schematic representation of using fluorophore-labeled (FAM)-ssDNA to detect the presence of a cDNA target through induced desorption from the GO surface. (B) Fluorescence quenching of probe DNA by adsorption (curve a) and restoration of the signal upon target DNA addition (curve b) as a function of time. Adapted from ref. 12 with permission from Wiley. (C) Hybridization induced desorption of probe DNA with cDNA or non-complementary DNA (nDNA) from CNTs as a function of time. Adapted from ref. 27 with permission from Europe PMC. (D) Fluorescent response of the desorption of FAM-DNA from AuNPs with cDNA or unmodified probe of the same sequence as the probe DNA (sDNA) before complete dissolution with KCN, as a function of time. Inset shows a close up of time points 0–20 min with a smaller *y*-axis scale. Adapted from ref. 16 with permission from the American Chemical Society.

significantly. For example, DNA adsorbs to NiO very strongly and can barely be displaced.[26]

When a duplex DNA or an aptamer binding complex is formed, the DNA bases are hidden inside and this can lead to a thermodynamic and/or kinetic disadvantage for adsorption to nanomaterials. Taking advantage of the adsorption interactions, biosensors are designed based on either target-induced DNA desorption or inhibited DNA adsorption. The assumption is that the DNA/target complex is adsorbed weaker or slower compared to free DNA probes. However, this assumption may not be true for all surfaces, especially for AuNPs that can strongly adsorb DNA. Some examples are illustrated below.

Surface-governed sensing performance

Fig. 1(A) shows the sensor design by Yang and coworkers using GO.[12] A fluorescently-labeled DNA oligomer was first adsorbed onto the GO surface to achieve fluorescence quenching. When the target cDNA was added, the fluorescence enhanced due to the presumed hybridization of the DNA forming a duplex that cannot be stably adsorbed onto GO. This simple and elegant design showed remarkable analytical performance with over 30-fold fluorescence enhancement, and around 80% of signal generation occurring in 5 min (Fig. 1(B)). The success of the GO-based sensors has inspired a lot of interest, and similar designs can be found with essentially any type of nanomaterial, since most nanomaterials can effectively adsorb DNA and quench adsorbed fluorophores.

While the same reaction scheme can be drawn, not every nanomaterial would work the same way. For example, signal generation using carbon nanotubes (CNTs) was much slower than using GO. In 2006, the Strano group monitored DNA hybridization utilizing the intrinsic fluorescence of CNTs, and it took around 13 h for the signal to saturate (Fig. 1(C)),[27] thus suggesting that CNTs are a suboptimal material for this application. Later, the Tan group studied the fluorescence signaling and quenching property of CNTs.[28] The reason that long incubation times are required to saturate the fluorescent response is because DNA can wrap around carbon nanotubes leading to a much stronger adsorption affinity compared to GO,[29] making it more difficult for cDNA to compete for the CNT surface.

Moreover, AuNPs are also excellent fluorescence quenchers. However, in our opinion, AuNPs do not work with this sensing scheme as shown in Fig. 1(A). This is because the interaction between AuNPs and DNA occurs *via* very strong DNA base coordination,[21,30,31] and this adsorption is even stronger than that on CNTs. It is well known that to immobilize thiolated DNA onto a gold electrode, it is important to backfill the surface with MCH to desorb nucleobases,[22] otherwise DNA hybridization would not occur.[21] The same strong interaction also exists between DNA and AuNPs. Our lab mixed 6-carboxyfluorescein (FAM)-labeled DNA with AuNPs, and washed away non-adsorbed DNA probes.[16] Due to the very strong adsorption and fluorescence quenching ability of AuNPs, adding cDNA can only increase the fluorescence by about 1-fold (Fig. 1(D)), which is much lower than what's observed for GO. Adding KCN to fully dissolve the AuNPs resulted in a fluorescence enhancement attributable to ~99% of the DNA still being adsorbed to the surface of the AuNPs.[16] Therefore, added cDNA can barely desorb DNA from AuNPs. For this target-induced desorption reaction scheme to work, the hybridization energy of the DNA to its target should be higher than the adsorption energy of the DNA to the substrate surface.

Mechanism of DNA surface reactions

For systems where this sensing reaction worked well, an interesting query to consider is the mechanism for which DNA

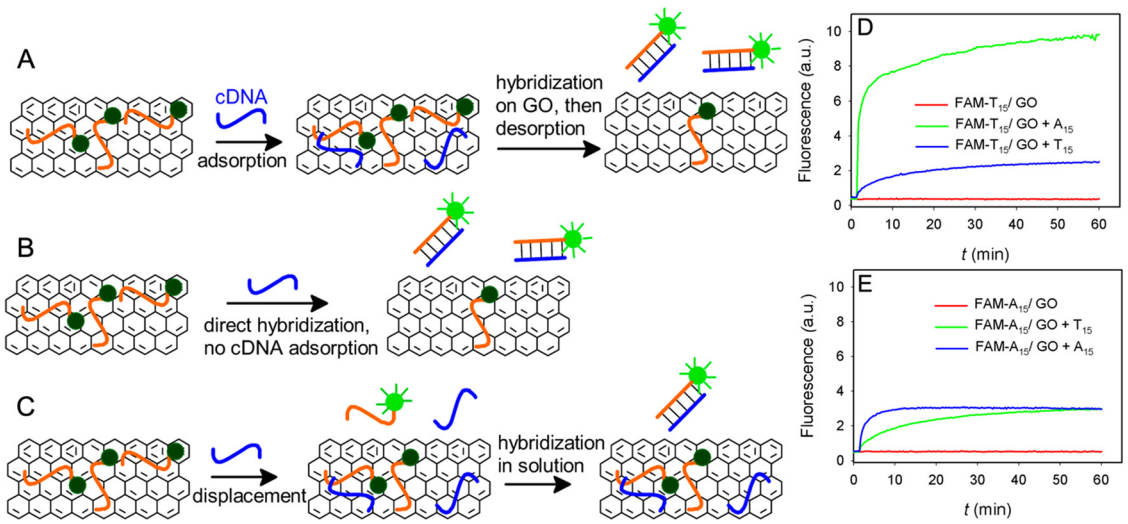

Fig. 2 Three possible mechanisms of probe DNA hybridization reacting with cDNA on a GO surface. (A) Langmuir–Hinshwood mechanism, (B) Eley–Rideal mechanism, and (C) displacement mechanism. Kinetics of fluorescent enhancement by DNA-induced desorption of (D) FAM-T_{15} and (E) FAM-A_{15} probe DNA from GO by various DNAs added at 1 min. Adapted from ref. 32 with permission from the American Chemical Society.

hybridization occurs. There are two main postulations in the literature about the mechanism of probe DNA and cDNA hybridization at a nanomaterials' surface: (i) the probe DNA and cDNA hybridize on the surface, and the formed duplex is then desorbed (Langmuir–Hinshwood mechanism, Fig. 2(A)), and (ii) the cDNA in solution directly hybridizes with the adsorbed DNA (Eley–Rideal mechanism, Fig. 2(B)). These mechanisms both imply that the hybrid DNA complex is more stable than the probe DNA/nanomaterial interactions. However, there is no mention to the affinity of the cDNA to the nanomaterial surface. To address this, our lab did some fundamental studies using poly-A and poly-T DNA as probes on a GO surface.[32] It is known that poly-A adsorption is stronger than poly-T adsorption on GO.[33,34] We observed that the reaction was always faster when poly-A was used for probe desorption (Fig. 2(D) and (E)). Therefore, at least for poly-A and poly-T DNA, the mechanism is displacement of adsorbed probe DNA by cDNA followed by hybridization to excess cDNA in solution. In this case, the more favourable adsorption of poly-A displaces poly-T from the GO surface (Fig. 2(C)). We found that the binding affinities increased in the order of poly-A/GO $\gg$ poly-T/GO $>$ poly-A/poly-T, supporting our displacement mechanism. Furthermore, each DNA sequence is different. For example, we found that at neutral pH, poly-C DNA has the strongest affinity to GO,[33] and this was later attributed to the lack of stable secondary structures of poly-C DNA at neutral pH.[35] At low pH, the affinity of poly-C is actually weaker. For the sensing scheme in Fig. 1(A) to work, it is important to have the surface adsorption affinity of both probe DNA and cDNA comparable with DNA hybridization, so that the adsorbed DNA can still be released.

Given a high possibility of artifacts, control experiments are extremely important. A reliable control is to change the DNA sequence while still keeping a similar base composition. With a similar base composition, the adsorption affinity to nanomaterials should be similar. If a nonbinding mutant shows a similar amount of signal change as the original sequence, then it is likely that the observed change is due to nonspecific events instead of the intended hybridization or aptamer binding.

Probe desorption due to target adsorption

The above DNA sensing mechanism on GO already indicated the effect of target adsorption to nanomaterials, and competition with pre-adsorbed probe DNA.[32] When DNA is used as a target, it is quite easy to understand that target DNA may compete with probe DNA. For many aptamer targets, their interactions with surfaces are less obvious. The effect of target adsorption can be exemplified by the colorimetric sensing of arsenic as detailed below.

A 100-nucleotide long arsenic binding aptamer, known as Ars-3, was reported by Kim *et al.* in 2009.[36] The characterization of aptamer binding was achieved using surface plasmon resonance (SPR) by immobilizing arsenic onto a gold surface. This paper claimed a similar low nM binding affinity to both As(III) and As(V). Many of the subsequent biosensor papers using Ars-3 employed AuNPs, but those papers could only detect As(III), not As(V).[37,38] Some sensors were designed based on the scheme shown in Fig. 3(A), where aptamer binding to As(III) inhibited its adsorption to AuNPs, subsequently inducing particle

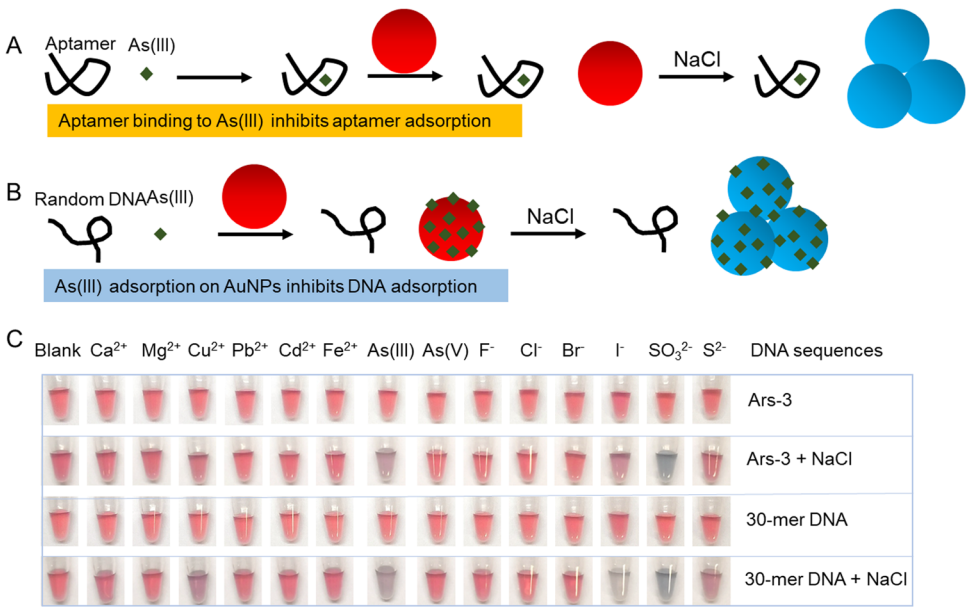

Fig. 3 Schematic representation of two possible mechanisms of AuNP aggregation induced by NaCl. (A) The Ars-3 DNA binding to As(III) to inhibit DNA adsorption to AuNPs, and (B) As(III) adsorption directly to AuNPs to inhibit DNA adsorption to AuNPs. Adapted from ref. 40 with permission from the American Chemical Society. (C) Colorimetric response of AuNP aggregation as induced by mixing of AuNPs with Ars-3 or a 30-mer DNA sequence, together with the addition of NaCl. Adapted from ref. 39 with permission from the American Chemical Society.

aggregation in the presence of NaCl. How is it possible then that for the same aptamer, it can bind both As(III) and As(V) in one method, while it can only bind to As(III) in the other? While we could reproduce the literature results with Ars-3, we also observed the same with other DNA sequences (Fig. 3(C)), suggesting that the color change in the presence of As(III) was independent of DNA sequence. After extensive studies, we cannot find any evidence supporting specific binding of As(III) or As(V) by this DNA sequence, and we present sufficient data showing that Ars-3 is not actually an aptamer for arsenic.[39] These observations were rationalized by the scheme shown in Fig. 3(B), where As(III), but not As(V), can readily adsorb onto the AuNP surface to inhibit DNA adsorption and permit AuNP aggregation by NaCl.[40] This is also true for several anionic species including I^-, SO_3^{2-}, and S^{2-} (Fig. 3(C)); most previous studies only compared As(III) with metal cations but did not include anions. When SPR was used, both As(III) and As(V) showed binding. The signal produced was probably due to the nonspecific adsorption of DNA to the gold surface.

Metal oxide nanoparticles

In an attempt to avoid the issues regarding the dominating effect of surface–target interactions out-competing probe–target interactions as seen with AuNPs, we used metal oxide nanoparticles (MONPs).[41] The detection of adenosine (Ade) and ATP was compared using its aptamer in a method equivalent to that as shown in Fig. 1(A). In contrast to AuNPs, DNA interacts with MONPs through its negatively charged phosphate backbone as opposed to base coordination. Using FAM-labeled aptamer and CeO_2 NPs, only ATP produced a concentration-dependent response (Fig. 4(A)). In addition, this response was also reproducible using a non-specific A_{15} probe (Fig. 4(B)), and with GTP. Finally, similar observations were also made with other MONPs including ZnO, NiO, Fe_3O_4, and TiO_2. These results support that even for MONPs, target adsorption out-competes aptamer–target binding interactions.

Interestingly, using GO in the same method yielded a slightly more selective detection for adenosine in comparison to ATP (Fig. 4(C)). However, there was still weak affinity of the GO surface to ATP, GTP, and guanosine (Gua), whereas thymidine and cytosine did not displace any aptamer probes from the GO surface.

In a direct comparison of GO and MONP sensors, we measured the DNA desorption of GO compared to NiO MONPs using bovine serum albumin (BSA, a representative protein found abundantly in biological samples) and cDNA. The GO sensor desorbed 30% of the probe DNA in the presence of BSA, which was otherwise barely detectable using NiO MONPs (Fig. 4(D) and (E)), producing a signal-to-noise ratio 12-fold greater for MONPs compared to GO. This result was attributed to the fact that most proteins do not have a competing phosphate group, where DNA adsorption to MONPs relies mainly on its phosphate backbone. Thus, there is a lack of competing species in the sample as opposed to using GO, where proteins are able to sufficiently desorb probe DNA.[42]

With the above discussion, these nanomaterials (AuNPs, MONPs, GO) can be classified based on their interaction strength with DNA, represented as very strong (Fig. 5(A)), strong (Fig. 5(B)),

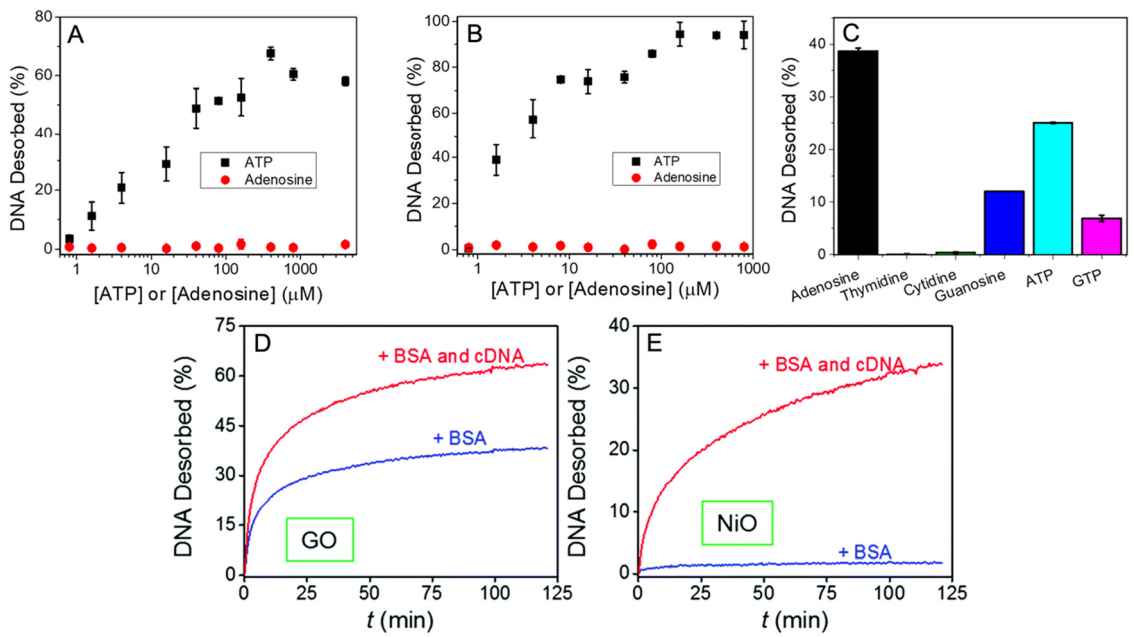

Fig. 4 Concentration-dependent response of fluorescently-labeled-aptamer-coated CeO_2 NPs upon addition of ATP and Ade using the (A) Ade/ATP aptamer or (B) A_{15} oligonucleotide. (C) Fluorescent response using fluorescently-labeled aptamer on a GO surface with the addition of various target analytes. Adapted from ref. 41 with permission from the American Chemical Society. Fluorescent response of desorbed probe DNA induced by BSA or BSA + cDNA using (D) GO and (E) NiO as a function of time. Adapted from ref. 42 with permission from the Royal Society of Chemistry.

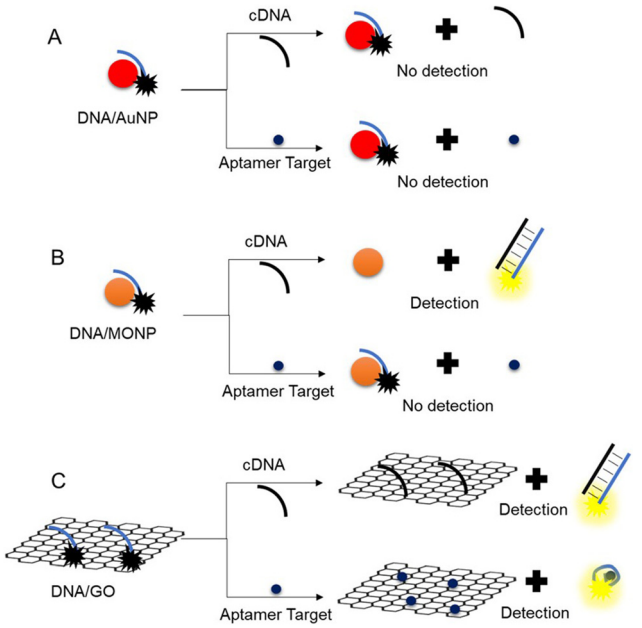

Fig. 5 Classification of nanomaterials based on their relative strength of DNA adsorption. (A) AuNPs adsorb DNA very strongly, where even cDNA cannot induce desorption. (B) MONPs adsorb DNA relatively strongly, where cDNA can induce desorption but aptamer targets cannot. (C) GO adsorbs DNA with moderate strength, where both cDNA and aptamer targets can induce desorption. Adapted from ref. 41 with permission from the American Chemical Society.

and moderate (Fig. 5(C)).[41] For AuNPs, its interaction with DNA is much stronger than DNA hybridization interactions. For some MONPs, DNA hybridization can compete with DNA adsorption, but aptamer binding may not be strong enough to compete. For GO, even aptamer binding to its target may compete with aptamer adsorption.

Label-free colorimetric sensing using gold nanoparticles

AuNPs are at the foundation of colorimetric sensing due to their unique and remarkable distant-dependent optical properties.[1,43] Additionally, it is well known that ssDNA has a much higher efficiency of adsorption to the AuNP surface than that of dsDNA.[21,44] With this knowledge, a label-free method of colorimetric sensing was reported by Li and Rothberg in 2004.[10,11] This method relies on mixing an unmodified probe (DNA lacking a thiol group) with the target analyte before adsorbing onto the AuNPs, and has since expanded to the detection of aptamer targets (Fig. 6(A)). At the time of writing, nearly 800 aptamer sequences are available from the publicly available Apta-Index™ (aptagen.com). Our lab has carefully examined a few aptamers to validate the sensing mechanism. Two examples of using aptamers for label-free colorimetric sensing are described below for Ade and dopamine.

In 1995, the Szostak lab described an aptamer for Ade with a K_d of 6 μM. Its affinity for AMP and ATP was slightly weaker, while no binding was reported for the other ribonucleosides including Gua, uridine, or cytosine. This aptamer was tested with the label-free method as shown in Fig. 6(A) using four analytes including Ade, ATP, Gua, and GTP.[45] Interestingly, only ATP produced a concentration-dependent colorimetric response (Fig. 6(B)), in contrast to the reported stronger binding affinity of the aptamer to Ade compared to ATP. These

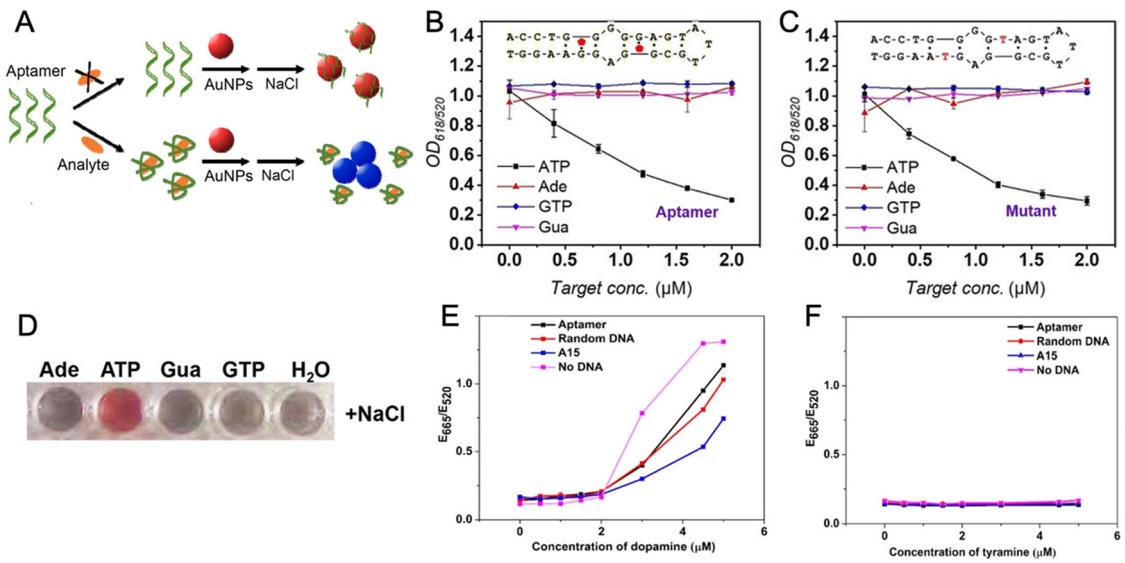

Fig. 6 (A) Schematic representation of label-free colorimetric sensing which relies on the inhibition of aptamer adsorption on AuNPs through binding with a suitable analyte. Colorimetric response of AuNP aggregation induced by analyte addition to AuNPs with (B) the Ade/ATP aptamer or (C) a non-binding mutant aptamer. (D) Photograph of AuNPs mixed with the Ade/ATP aptamer and addition of respective analyte and NaCl. Adapted from ref. 45 with permission from the American Chemical Society. Colorimetric response of AuNP aggregation induced by (E) dopamine and (F) tyramine in the presence of various DNA sequences. Adapted from ref. 48 with permission from Chemistry Europe.

results were also reproduced using a non-binding mutant aptamer (Fig. 6(C)). It was concluded that the phosphate groups present on ATP are able to induce a stabilizing effect against AuNP aggregation, even in the presence of aggregation-inducing NaCl (Fig. 6(D)). For GTP, no protection was observed due to the lower affinity of Gua to the Au surface in comparison to Ade.

In 2018, Stojanović and co-workers reported a DNA aptamer for dopamine;[46] which has nanomolar affinity.[47] Using the same method (Fig. 6(A)), the dopamine aptamer was tested along with three controls including a random DNA sequence, A_{15}, and no DNA.[48] Aggregation of AuNPs was induced in the presence of dopamine (Fig. 6(E)) but not tyramine (Fig. 6(F)), regardless of the DNA sequence used. Previous studies have identified the ability of dopamine to adsorb onto Au, with a very strong apparent binding affinity of K_d = 5.8 μM, based on AuNP aggregation.[49] The observed color change with dopamine was due to its stronger ability to induce the aggregation of AuNPs compared to tyramine.

These two examples described here, representing only a few of many in the literature, demonstrate how target adsorption can dominate aptamer binding and interfere with the label-free colorimetric method of sensing. While different target molecules may interact differently with AuNPs, it is important to consider each case carefully.

The only example where label-free colorimetric sensing has worked for the detection of a small molecule is for the detection of K^+.[49] Still, for the practical use of label-free colorimetric sensing, the composition of the sample matrix must be considered. While the detection for K^+ is possible, its practicality is still questionable considering that environmental and biological samples will contain many types of analytes that can interact with the AuNP surface. As summarized by Zhang and Liu,[48] and depicted in Fig. 7, target analytes can be categorized into four classes. Briefly, class 1 analytes adsorb to AuNPs causing destabilization of colloidal particles and a subsequent color change (*e.g.* dopamine, adenosine); class 2 analytes can adsorb onto AuNPs without any significant affect (*e.g.* As(III)); class 3 analytes adsorb to AuNPs causing stabilization and inhibit any subsequent color change (*e.g.* ATP); and class 4 analytes have no discernable affect (*e.g.* K^+). Only class 4 analytes can be detected using this method.

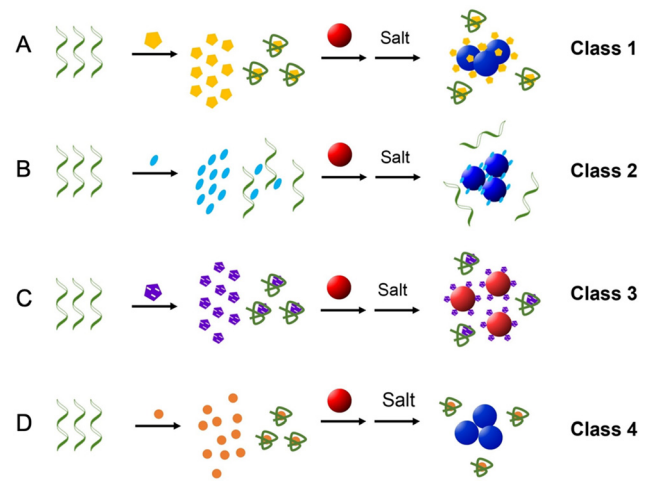

Fig. 7 Categorization of target analytes based on their interaction with AuNPs. (A) Adsorb onto AuNP and lead to destabilization (*e.g.* dopamine, adenosine), (B) adsorb onto AuNPs with little stabilization or destabilization affects (*e.g.* As(III)), (C) adsorb onto AuNPs and lead to stabilization (*e.g.* ATP), and (D) do not adsorb onto AuNPs and have no discernable affects (*e.g.* K^+). Reproduced from ref. 48 with permission from Chemistry Europe.

Covalent *versus* noncovalent sensors

For the DNA–AuNP system, using thiolated DNA to covalently attach the target probe can give a more specific response since in that case, only the optical property of AuNPs (color change or fluorescence quenching) is utilized instead of its surface properties.[1] Additionally, using a covalent linkage is more reliable in the DNA–GO system in terms of resisting nonspecific displacement of the target probe.[50] For example, we constructed a covalent GO sensor using a fluorescently-labeled DNA probe covalently attached to GO.[50] Still, the heterogeneity of the GO surface can lead to various microenvironments where either covalent attachment or adsorption can dominate. To resolve this, the conjugated GO needed to be washed to desorb any non-covalent, physisorbed probe DNA. To achieve this, cDNA lacking a fluorescent label was incubated with the functionalized GO sensor. As seen in Fig. 8(A), the cDNA was sufficient to desorb all adsorbed probe DNA from the surface, as represented by a non-fluorescent supernatant after an additional wash step, and centrifugation of the GO. Only the GO pellet was slightly fluorescent, indicating that all fluorophores were covalently associated with GO, thus successfully producing a functional covalent sensor. In contrast, all probe DNA washed from a non-covalent sensor remained in the supernatant after centrifugation (Fig. 8(B)). Next, both the covalent and non-covalent sensors were tested for their ability to detect target DNA (Fig. 8(C)–(E)). Using cDNA to test detection, and the same DNA (probe DNA lacking a fluorescent label) to test for non-specific probe displacement, the covalent sensor was able to adequately discern the two (Fig. 8(C)). In contrast, the non-covalent sensor was susceptible to nonspecific probe displacement (Fig. 8(D)), even with a reduced concentration of probe DNA (Fig. 8(D) inset) – a common method to reduce this effect. To show its practicality, a sample matrix comprised of 0.5% BSA was exposed to each sensor (Fig. 8(E)). The covalent sensor had a sharp and small increase in fluorescent signal followed by stabilization of the response, whereas the non-covalent sensor had a long increasing response over time. These results are consistent with the non-specific displacement of probe DNA from non-covalent sensors, and highlight the benefits of covalent attachment.

When competitive adsorption exists, nonspecific interactions are often possible. So, for developing practical sensors, we believe that using covalently-conjugated DNA probes is a more reliable method. However, it should be noted that with

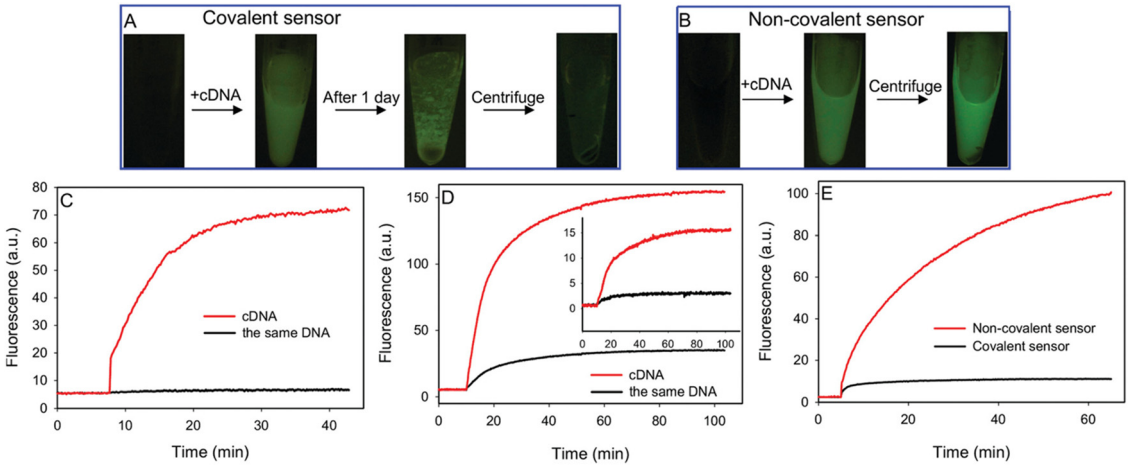

Fig. 8 Photographs of fluorescence associated with GO sensors prepared using covalent (A) and non-covalent (B) DNA probes after washing with cDNA and centrifugation. Fluorescent response of the covalently (C) and non-covalently (D) prepared GO sensors after the addition of cDNA and same-DNA (probe DNA lacking a fluorescent label). The inset of panel (D) is with 10-fold less probe DNA. (E) Fluorescent response of the covalently and non-covalently prepared GO sensors in the presence of 0.5% BSA. Reproduced from ref. 50 with permission from the American Chemical Society.

the covalent attachment of DNA probes, the advantage of simplicity is lost. In addition, physisorption-based biosensors can be used to study aptamer binding, or target/aptamer, and target/nanomaterial interactions, in well-controlled systems. To validate proposed sensing mechanisms, the functionality of the assay has to be established by using carefully designed control sequences.

Summary and future perspectives

With thousands of papers published over nearly three decades, and a plethora of interesting nanomaterials having been interfaced with DNA, the field of DNA/nanomaterial-based biosensors should have already passed the proof-of-concept stage. This article is mainly focused on biosensors utilizing physisorbed DNA or aptamer probes. Based on our observation, there is not yet a single material that is sufficiently robust to allow such adsorption-based probes to be reliable for practical applications. These sensors suffer from nonspecific displacement from proteins and other nucleic acids and even small molecules, and this will be a major problem in complex sample matrix. Many of the observed fluorescence or color changes did not reflect aptamer binding, but rather through other events such as target adsorption. This is of most concern for label-free AuNP-based detection as reviewed in this article. As summarized in Table 1, and illustrated in Fig. 9, these mechanistic problems exist for different types of biosensor designs based on either target-induced probe DNA desorption or inhibited probe DNA adsorption. The undesired desorption (or inhibited adsorption) of probe DNA *via* the preferential adsorption of the target DNA or small molecule can lead to alternative and non-specific mechanisms of signal generation. Thus, as mentioned previously, each case must be considered carefully, and the use of proper controls is essential to establish a practical and reproducible biosensor design.

Table 1 Summary of the different types of nanomaterials reviewed in this article and their ability, or lack-there-of, to provide a reliable signal for the given mechanism of signal generation

Mechanism	Target-induced probe desorption		Target-inhibited probe adsorption	
Target	DNA	Small molecules	DNA	Small molecules
GO	✓	✓	✓	✓
AuNPs	✗	✗	✓	?
Metal oxides	✓	?	✓	?

For the cases where the sensing mechanism is valid, sample matrix effects, such as competition from proteins, may also mislead the analytical results. In some special cases, for

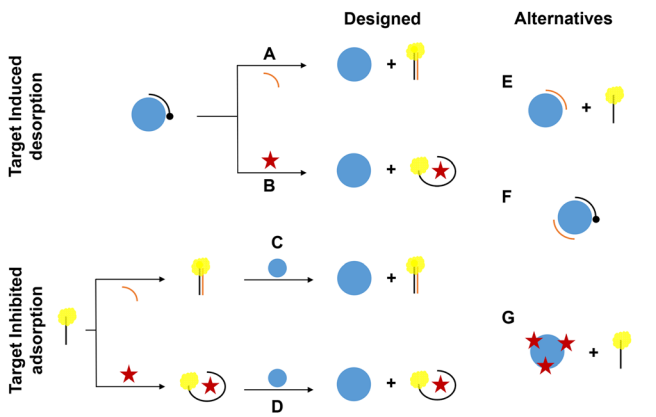

Fig. 9 Illustrative summary of the types of signal generation by target-induced desorption and target-inhibited adsorption. Desorption of the DNA probe can be induced by the addition of (A) cDNA, or (B) a small molecule target. Likewise, adsorption of the DNA probe can be inhibited by (C) cDNA, or (D) a small molecule target. Alternative mechanisms to these biosensor designs can be through (E) displacement of the probe DNA by preferential cDNA adsorption producing a non-specific signal, (F) adsorption of target cDNA without signal generation, and/or (G) displacement of the probe DNA by preferential adsorption of a small molecule target producing a non-specific signal.

example, the monitoring of DNA in PCR or loop-mediated isothermal amplification (LAMP) products, these sensing mechanisms may prove useful, although alternative solutions such as DNA staining dyes are available.

For future studies, we have a few recommendations. First, we recommend to use such systems as a research tool for fundamental DNA/materials interface studies. One can learn about interactions between target molecules and inorganic nanomaterials using the fluorescence change of DNA or color change of AuNPs as a measurable response. These studies may not lead to practically useful biosensors, but they can help to gain fundamental understandings and avoid making mistakes in subsequent biosensor development. Second, to really develop practical biosensors, we need to first analyze the sample matrix and identify main competitors. In environmental water, the interference could arise from simple ions, whereas in biological samples, proteins are more problematic. Since each sample matrix is different, it is useful to find one or a few important model systems for optimization. For example, blood serum has a high content of proteins, and surfaces that stably adsorb DNA in the presence of proteins are needed. We discovered that DNA adsorbed to some metal oxides are more resistant to displacement by proteins, but they are more susceptible to phosphate.[42] In contrast, DNA adsorbed on GO is insensitive to phosphate, but they are easily displaced by proteins. It is probably impossible to have a system that can work in all sample matrixes, but if we define the sample, optimization should be simpler. Finally, with sufficient understanding, efforts can be made to design biosensors with broader applicability or to develop multiple optimized systems tailored for specific sample matrixes.

Conflicts of interest

There are no conflicts to declare.

Acknowledgements

Funding for this work was from the Natural Sciences and Engineering Research Council of Canada (NSERC).

References

1 N. L. Rosi and C. A. Mirkin, *Chem. Rev.*, 2005, **105**, 1547–1562.
2 C. R. Laramy, M. N. O'Brien and C. A. Mirkin, *Nat. Rev. Mater.*, 2019, **4**, 201–224.
3 J. Li, L. Mo, C.-H. Lu, T. Fu, H.-H. Yang and W. Tan, *Chem. Soc. Rev.*, 2016, **45**, 1410–1431.
4 L. L. Li, H. Xing, J. J. Zhang and Y. Lu, *Acc. Chem. Res.*, 2019, **52**, 2415–2426.
5 Q. Hu, H. Li, L. Wang, H. Gu and C. Fan, *Chem. Rev.*, 2019, **119**, 6459–6506.
6 C. A. Mirkin, R. L. Letsinger, R. C. Mucic and J. J. Storhoff, *Nature*, 1996, **382**, 607–609.
7 R. Elghanian, J. J. Storhoff, R. C. Mucic, R. L. Letsinger and C. A. Mirkin, *Science*, 1997, **277**, 1078–1080.
8 S. P. Song, Y. Qin, Y. He, Q. Huang, C. H. Fan and H. Y. Chen, *Chem. Soc. Rev.*, 2010, **39**, 4234–4243.
9 L. H. Tan, H. Xing and Y. Lu, *Acc. Chem. Res.*, 2014, **47**, 1881–1890.
10 H. Li and L. Rothberg, *Proc. Natl. Acad. Sci. U. S. A.*, 2004, **101**, 14036–14039.
11 H. Li and L. J. Rothberg, *J. Am. Chem. Soc.*, 2004, **126**, 10958–10961.
12 C. H. Lu, H. H. Yang, C. L. Zhu, X. Chen and G. N. Chen, *Angew. Chem., Int. Ed.*, 2009, **48**, 4785–4787.
13 C. Zhu, Z. Zeng, H. Li, F. Li, C. Fan and H. Zhang, *J. Am. Chem. Soc.*, 2013, **135**, 5998–6001.
14 B. Liu and J. Liu, *TrAC, Trends Anal. Chem.*, 2019, **121**, 115690.
15 B. Liu, S. Salgado, V. Maheshwari and J. Liu, *Curr. Opin. Colloid Interface Sci.*, 2016, **26**, 41–49.
16 F. Zhang, S. Wang and J. Liu, *Anal. Chem.*, 2019, **91**, 14743–14750.
17 H. Wang, R. H. Yang, L. Yang and W. H. Tan, *ACS Nano*, 2009, **3**, 2451–2460.
18 H. Pei, X. L. Zuo, D. Zhu, Q. Huang and C. H. Fan, *Acc. Chem. Res.*, 2014, **47**, 550–559.
19 J. J. Storhoff, R. Elghanian, C. A. Mirkin and R. L. Letsinger, *Langmuir*, 2002, **18**, 6666–6670.
20 B. Liu and J. Liu, *Matter*, 2019, **1**, 825–847.
21 T. M. Herne and M. J. Tarlov, *J. Am. Chem. Soc.*, 1997, **119**, 8916–8920.
22 B. Liu, P. Wu, Z. Huang, L. Ma and J. Liu, *J. Am. Chem. Soc.*, 2018, **140**, 4499–4502.
23 H. D. Hill, J. E. Millstone, M. J. Banholzer and C. A. Mirkin, *ACS Nano*, 2009, **3**, 418–424.
24 J. S. Park, H.-K. Na, D.-H. Min and D.-E. Kim, *Analyst*, 2013, **138**, 1745–1749.
25 B. Liu and J. Liu, *ACS Appl. Mater. Interfaces*, 2015, **7**, 24833–24838.
26 L. Chen, B. Liu, Z. Xu and J. Liu, *Langmuir*, 2018, **34**, 9314–9321.
27 E. S. Jeng, A. E. Moll, A. C. Roy, J. B. Gastala and M. S. Strano, *Nano Lett.*, 2006, **6**, 371–375.
28 R. H. Yang, J. Y. Jin, Y. Chen, N. Shao, H. Z. Kang, Z. Xiao, Z. W. Tang, Y. R. Wu, Z. Zhu and W. H. Tan, *J. Am. Chem. Soc.*, 2008, **130**, 8351–8358.
29 X. Tu, S. Manohar, A. Jagota and M. Zheng, *Nature*, 2009, **460**, 250–253.
30 J. Liu, *Phys. Chem. Chem. Phys.*, 2012, **14**, 10485–10496.
31 J. M. Carnerero, A. Jimenez-Ruiz, P. M. Castillo and R. Prado-Gotor, *ChemPhysChem*, 2017, **18**, 17–33.
32 B. Liu, Z. Sun, X. Zhang and J. Liu, *Anal. Chem.*, 2013, **85**, 7987–7993.
33 C. Lu, Z. Huang, B. Liu, Y. Liu, Y. Ying and J. Liu, *Angew. Chem., Int. Ed.*, 2017, **56**, 6208–6212.
34 N. Varghese, U. Mogera, A. Govindaraj, A. Das, P. K. Maiti, A. K. Sood and C. N. R. Rao, *ChemPhysChem*, 2009, **10**, 206–210.

35 A. Lopez, Y. Zhao, Z. Huang, Y. Guo, S. Guan, Y. Jia and J. Liu, *Adv. Mater. Interfaces*, 2021, **8**, 2001798.
36 M. Kim, H. J. Um, S. Bang, S. H. Lee, S. J. Oh, J. H. Han, K. W. Kim, J. Min and Y. H. Kim, *Environ. Sci. Technol.*, 2009, **43**, 9335–9340.
37 K. Matsunaga, Y. Okuyama, R. Hirano, S. Okabe, M. Takahashi and H. Satoh, *Chemosphere*, 2019, **224**, 538–543.
38 Y. Wu, S. Zhan, H. Xing, L. He, L. Xu and P. Zhou, *Nanoscale*, 2012, **4**, 6841–6849.
39 C. Zong and J. Liu, *Anal. Chem.*, 2019, **91**, 10887–10893.
40 C. Zong, Z. Zhang, B. Liu and J. Liu, *Langmuir*, 2019, **35**, 7304–7311.
41 A. Lopez and J. Liu, *Anal. Chem.*, 2021, **93**, 3018–3025.
42 B. Liu, L. Ma, Z. Huang, H. Hu, P. Wu and J. Liu, *Mater. Horiz.*, 2018, **5**, 65–69.
43 K. Saha, S. S. Agasti, C. Kim, X. Li and V. M. Rotello, *Chem. Rev.*, 2012, **112**, 2739–2779.
44 F. Li, H. Pei, L. Wang, J. Lu, J. Gao, B. Jiang, X. Zhao and C. Fan, *Adv. Funct. Mater.*, 2013, **23**, 4140–4148.
45 F. Zhang, P.-J. J. Huang and J. Liu, *ACS Sens.*, 2020, **5**, 2885–2893.
46 N. Nakatsuka, K.-A. Yang, J. M. Abendroth, K. M. Cheung, X. Xu, H. Yang, C. Zhao, B. Zhu, Y. S. Rim, Y. Yang, P. S. Weiss, M. N. Stojanović and A. M. Andrews, *Science*, 2018, **362**, 319–324.
47 X. Liu, Y. Hou, S. Chen and J. Liu, *Biosens. Bioelectron.*, 2020, 112798.
48 F. Zhang and J. Liu, *Analysis Sensing*, 2021, **1**, 30–43.
49 X. Liu, F. He, F. Zhang, Z. Zhang, Z. Huang and J. Liu, *Anal. Chem.*, 2020, **92**, 9370–9378.
50 P.-J. J. Huang and J. Liu, *Anal. Chem.*, 2012, **84**, 4192–4198.